

Supplementary Information: Stellar population synthesis modeling

The stellar population model used in the present analysis was constructed specifically for this project. We therefore describe it in some detail below.

Construction of the model:

The IRTF spectral library^{13,31} constitutes the core of our model. This spectral library is novel in its near-IR coverage of a large sample of cool stars at a resolving power of $R \sim 2000$. 65 stars were selected from this library with luminosity classes III and V (giants and dwarfs). Peculiar stars were removed, including stars with non-solar Fe abundance and/or other peculiar abundance patterns (mainly Ca, CN, CH, and Ba), as well as known pulsating M giants. Stars with significant reddening were also removed. The IRTF library includes 2MASS *JHK* and literature *V* band photometry for each star.

We estimated effective temperatures for these stars based on empirical $V - K$ vs. T_{eff} relations that have been separately determined for giants^{32–34} and dwarfs.^{35,36} The adopted dwarf relations agree to within 100 K with a recently updated temperature scale.^{37,38}

The IRTF library is absolute-flux calibrated against 2MASS photometry. We adopt parallax values obtained from SIMBAD in order to derive absolute luminosities. In order to derive bolometric luminosities, which we will use to assign stellar masses, we must extrapolate the IRTF library beyond the observed range. We perform the extrapolation by utilizing the latest version of the PHOENIX model spectra. The model spectra are normalized to the IRTF library at the blue and red ends of the observed wavelength range so that the extrapolation is continuous across the transition region. The model spectrum used to extrapolate each IRTF stellar spectrum was chosen from the estimated T_{eff} for each IRTF star and an estimate of the surface gravity of the star based on its luminosity class. We note that the extrapolation does not lead to large uncertainties as the IRTF wavelength range ($0.8 - 2.5 \mu\text{m}$) encompasses the majority of the bolometric flux, especially for K and M stars. As an example, 80% of the flux from M-type stars is emitted within the IRTF spectral range.

The resulting T_{eff} and L_{bol} for each IRTF star is plotted in Supp. Fig. 1. Also shown in this Figure are model isochrones (described below). The agreement between the data and models is remarkable, and provides a valuable consistency check on both the estimated T_{eff} and L_{bol} values.

We adopt a combination of isochrones in order to utilize the most accurate stellar models for each range in stellar mass. At the lowest masses we adopt the Baraffe stellar evolution calculations,³⁹ which are unique in their use of realistic atmospheric boundary conditions. Between $0.2 M_{\odot}$ and the tip of the RGB we use the Dartmouth evolutionary calculations,⁴⁰ which have been shown to produce accurate fits to photometry of open and globular clusters of a variety of ages and metallicities.⁴¹ The Padova evolutionary tracks⁴² are used to extend the isochrones through the horizontal branch and asymptotic giant branch evolutionary phases. This combined isochrone set is shown in Supp. Fig. 1.

The isochrones are used to assign masses to each IRTF spectrum, based on the measured L_{bol} for each star. We note that the stellar T_{eff} values are used only to choose the appropriate PHOENIX model spectra to extrapolate the observed spectra. Our conclusions remain unchanged if we instead assign masses based on the estimated T_{eff} for each star. Alpha-enhancements of 0.2 dex have a very minor effect on the $L_{\text{bol}} - M$ and $T_{\text{eff}} - M$ relations, when $[\text{Fe}/\text{H}]$ is held constant. As a final test of our procedure we compare the masses to those

predicted from empirical relations between mass and K -band luminosity derived for stars in binary systems.^{43,44} Such relations are completely independent of stellar evolution calculations because the masses are derived from dynamical modeling. The stellar mass – K -band luminosity relation for our IRTF stars agrees very well with the relations based on dynamical masses in the range $0.08 < M < 0.6 M_{\odot}$. The agreement is particularly strong when bolometric luminosities are used to assign masses, which motivates the use of bolometric luminosities as our default method. Based on these comparisons, we conclude that our mass estimates are reliable.

Once masses are assigned, a synthesized spectrum is created by integrating the observed spectra over an initial mass function.

Metallicity and α -enhancement:

The empirical spectral library that we use has important advantages over libraries of model atmospheres. Model atmospheres do not reproduce molecular features such as TiO very well, which makes it difficult to interpret fits of these models to our spectra. We note here that Kurucz models — which are used in most existing stellar population synthesis models at $\lambda > 8000 \text{ \AA}$ — also prefer IMFs that are more “bottom-heavy” than the Kroupa IMF, but give much poorer fits than the IRTF empirical library to the spectral regions away from Na I and the Wing-Ford band.

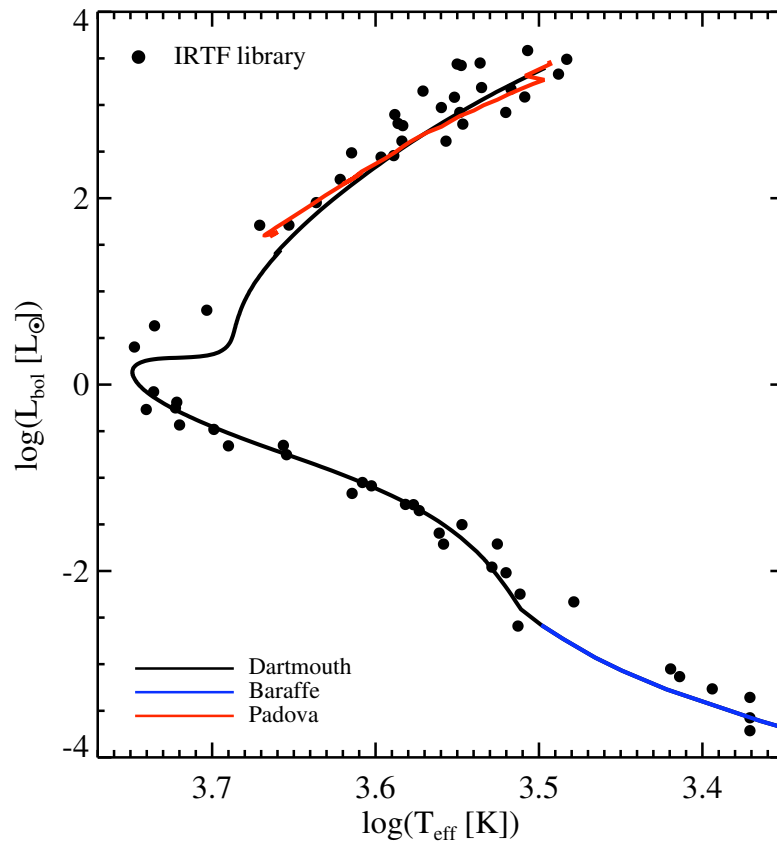
A disadvantage of the empirical library is that it is not straightforward to assess the effects of abundance variations. We know that the iron abundance in the eight Coma and Virgo ellipticals is approximately Solar,^{45,46} and so the value of $[\text{Fe}/\text{H}]$ of the Milky Way stars is appropriate for the galaxies that we study here. However, the abundance of α -elements (and the overall mass-weighted metallicity $[Z/\text{H}]$) is higher in massive elliptical galaxies than in the Milky Way stars. Although sodium (responsible for the Na I line) and iron (responsible for the Wing-Ford band) are themselves not α -elements, both lines and their sidebands overlap with TiO lines that are present in M giants.

We empirically determined to what extent enhanced TiO absorption could influence the results by creating models with artificially enhanced late M giant light. The model shown in Supp. Fig. 2 has a Kroupa IMF and an additional contribution of late M giants amounting to 40% of the light at $0.9 \mu\text{m}$. This is an extreme model as these stars should contribute only a few percent to the light, but we use it here to assess the effects of enhancing TiO features. This model fits the observed strength of the Wing-Ford band quite well as it coincides with the $\delta(2 - 3)$ band of TiO. However, it also predicts that other TiO features are nearly as strong as the absorption at $0.99 \mu\text{m}$, which is clearly not the case. Moreover, the fit to the Na I line is not improved as the only relevant TiO feature is slightly redward of Na I, and the fit to the rest of the spectrum in the wavelength range $0.815 - 0.860 \mu\text{m}$ is unacceptable. We note that the apparently limited enhancement of TiO with respect to the Milky Way giants is consistent with the weak response of TiO to either metallicity or α -enhancement in the PHOENIX library and in stellar population synthesis models which explicitly include non-Solar abundance ratios.⁴⁷

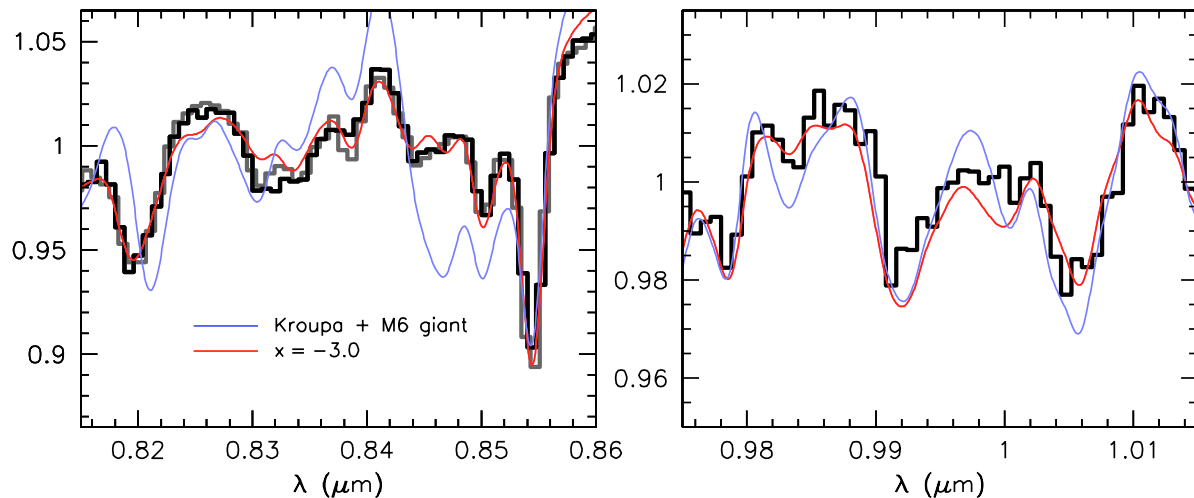
We infer that the Wing-Ford band should be interpreted with caution but that the combination of the Wing-Ford band with TiO features at other wavelengths and (particularly) the Na I line should be a robust indicator of the presence of low mass stars. This is fully consistent with previous theoretical work.³

31. Cushing, M. C., Rayner, J. T., & Vacca, W. D. An Infrared Spectroscopic Sequence of M, L, and T Dwarfs. *Astrophys. J.* **623**, 1115–1140 (2005)
32. Alonso, A., Arribas, S., & Martínez-Roger, C. The effective temperature scale of giant stars (F0-K5). II. Empirical calibration of T_{eff} versus colours and [Fe/H]. *Astron. Astrophys.* **140**, 261–277 (1999)
33. Perrin, G., Coudé du Foresto, V., Ridgway, S. T., Mariotti, J.-M., Traub, W. A., Carleton, N. P., & Lacasse, M. G. Extension of the effective temperature scale of giants to types later than M6. *Astron. Astrophys.* **331**, 619–626 (1998)
34. Ridgway, S. T., Joyce, R. R., White, N. M., & Wing, R. F. Effective temperatures of late-type stars - The field giants from K0 to M6. *Astrophys. J.* **235**, 126–137 (1980)
35. Alonso, A., Arribas, S., & Martinez-Roger, C. The empirical scale of temperatures of the low main sequence (F0V-K5V). *Astron. Astrophys.* **313**, 873–890 (1996)
36. Leggett, S. K., Allard, F., Berriman, G., Dahn, C. C., & Hauschildt, P. H. Infrared Spectra of Low-Mass Stars: Toward a Temperature Scale for Red Dwarfs. *Astrophys. J.* **104**, 117 (1996)
37. Casagrande, L., Flynn, C., & Bessell, M. M dwarfs: effective temperatures, radii and metallicities. *Mon. Not. R. Astron. Soc.* **389**, 585–607 (2008)
38. Casagrande, L., Ramírez, I., Meléndez, J., Bessell, M., & Asplund, K. An absolutely calibrated T_{eff} scale from the infrared flux method. Dwarfs and subgiants. *Mon. Not. R. Astron. Soc.* **512**, 54 (2010)
39. Baraffe, I., Chabrier, G., Allard, F., & Hauschildt, P. H. Evolutionary models for solar metallicity low-mass stars: mass-magnitude relationships and color-magnitude diagrams. *Astron. Astrophys.* **337**, 403–412 (1998)
40. Dotter, A., Chaboyer, B., Jevremović, D., Kostov, V., Baron, E., & Ferguson, J. W. The Dartmouth Stellar Evolution Database. *Astrophys. J. Supp.* **178**, 89–101 (2008)
41. An, D., Pinsonneault, M. H., Masseron, T., Delahaye, F., Johnson, J. A., Terndrup, D. M., Beers, T. C., Ivans, I. I., & Ivezić, Ž Galactic Globular and Open Clusters in the Sloan Digital Sky Survey. II. Test of Theoretical Stellar Isochrones. *Astrophys. J.* **623**, 523–544 (2009)
42. Marigo, P., Girardi, L., Bressan, A., Groenewegen, M. A. T., Silva, L., & Granato, G. L. Evolution of asymptotic giant branch stars. II. Optical to far-infrared isochrones with improved TP-AGB models. *Astron. Astrophys.* **482**, 883–905 (2008)
43. Henry, T. J. & McCarthy, Jr., D. W. The mass-luminosity relation for stars of mass 1.0 to 0.08 solar mass. *Astron. J.* **106**, 773–789 (1993)
44. Delfosse, X., Forveille, T., Ségransan, D., Beuzit, J.-L., Udry, S., Perrier, C., & Mayor, M. Accurate masses of very low mass stars. IV. Improved mass-luminosity relations. *Astron. Astrophys.* **364**, 217–224 (2000)

45. Trager, S. C., Faber, S. M., Worthey, G., & González, J. J. The Stellar Population Histories of Local Early-Type Galaxies. I. Population Parameters. *Astrophys. J.* **119**, 1645–1676 (2000)
46. Thomas, D., Maraston, C., Bender, R., & Mendes de Oliveira, C. The Epochs of Early-Type Galaxy Formation as a Function of Environment. *Astrophys. J.* **621**, 673–694 (2005)
47. Thomas, D., Maraston, C., & Bender, R. Stellar Population models of Lick indices with variable element abundance ratios. *Mon. Not. R. Astron. Soc.* **339**, 897–911 (2003)



Supplementary Figure 1 | The IRTF stellar library. Hertzsprung-Russell diagram of IRTF stars and theoretical stellar evolution calculations. IRTF stellar L_{bol} and T_{eff} have been estimated as described in the text. Theoretical models assume $[\text{Fe}/\text{H}] = 0.0$ and an age of 13.7 Gyr. The models encompass all phases of stellar evolution from main sequence hydrogen burning through the end of the asymptotic giant branch, and extend down to the hydrogen burning limit of $0.08 M_{\odot}$.



Supplementary Figure 2 | Effect of enhancing M giant features. **a** Spectra and models around the Na I doublet. Our favored model with a steep IMF ($x = -3.0$) is compared to a model that assumes a Kroupa IMF with the addition of a 40% light contribution from an M6 giant star. Since late M giants have very strong TiO features this exercise is meant to mimic the effects of increasing α -enhancement in the models. Clearly the addition of a substantial amount of M giant light provides a poor fit to the absorption line at $\approx 0.82 \mu\text{m}$ as the central wavelength is not matched. This demonstrates that this feature is due to Na I and not TiO. The fit is also very poor to the rest of the spectrum in this wavelength range. **b** Spectra and models around the Wing-Ford band. Here the addition of M giant light adequately reproduces the strong observed Wing-Ford absorption due to the TiO absorption feature that coincides with the FeH absorption. However, this fit also predicts unacceptably large absorption at $0.983 \mu\text{m}$, $1.001 \mu\text{m}$, and $1.006 \mu\text{m}$ as these TiO features are nearly as strong as the one at $0.992 \mu\text{m}$.